A single point mutation in the rhinovirus 2B protein reduces the requirement for phosphatidylinositol 4-kinase class 3beta in viral replication

Roulin, Pascal S ; Murer, Luca P ; Greber, Urs F

Abstract: Rhinoviruses (RVs) replicate on cytoplasmic membranes derived from the Golgi apparatus. They encode membrane-targeted proteins 2B, 2C and 3A, which control trafficking and lipid composition of the replication membrane. The virus recruits host factors for replication, such as the phosphatidylinositol 4 (PI4)-kinase 3beta (PI4K3b), which boosts PI4-phosphate (PI4P) levels, and drives lipid counter-current exchange of PI4P against cholesterol at endoplasmic reticulum-Golgi membrane contact sites through the lipid shuttling protein oxysterol binding protein (OSBP) 1. We identified a PI4K3b-inhibitor resistant RV-A16 variant with a single point mutation in the conserved 2B protein near the cytosolic carboxy-terminus, isoleucine 92 to threonine [I92T]. The mutation did not confer resistance to cholesterol sequestering compounds or OSBP1 inhibition, suggesting invariant dependency on the PI4P/cholesterol lipid counter-currents. In presence of PI4K3b-inhibitor, Golgi reorganization and PI4P lipid induction occurred in RV-A16 2B[I92], but not wild-type infection. The knock-out of PI4K3b abolished the replication of both 2B[I92T] mutant and wild-type. Doxycyclin-inducible expression of PI4K3b in PI4K3b knock-out cells efficiently rescued the 2B[I92T] mutant, and less effectively wild-type virus infection. Ectopic expression of 2B[I92T] or 2B was less efficient than 3A in recruiting PI4K3b to perinuclear membranes, suggesting a supportive rather than decisive role of 2B in recruiting PI4K3b. The data suggest that 2B tunes the recruitment of PI4K3b to the replication membrane, and allows the virus to adapt to cells with low levels of PI4K3b, yet maintaining the PI4P/cholesterol counter-current for establishing Golgi-derived RV replication membranes.Human rhinoviruses (RVs) are the major cause of common cold worldwide. They cause asthmatic exacerbations and chronic obstructive pulmonary disease. Despite recent advances, the development of antivirals and vaccines has proven difficult due to the high number and variability of RV types. The identification of critical host factors and their interactions with viral proteins and membrane lipids for the establishment of viral replication is a basis for drug development strategies. Our findings here shed new light on the interactions between nonstructural viral membrane proteins and class III phosphatidylinositol 4 kinases from the host, and highlight the importance of phosphatidyl-inositol 4 phosphate for RV replication.

DOI: https://doi.org/10.1128/JVI.01462-18

Roulin, Pascal S; Murer, Luca P; Greber, Urs F (2018). A single point mutation in the rhinovirus 2B protein reduces the requirement for phosphatidylinositol 4-kinase class 3beta in viral replication. Journal of Virology, 92(23):e01462-18.
DOI: https://doi.org/10.1128/JVI.01462-18

A single point mutation in the rhinovirus 2B protein reduces the requirement for phosphatidylinositol 4-kinase class 3beta in viral replication

Pascal S Roulin[1*], Luca Murer[1]*, Urs F Greber[1,2]

[1] Department of Molecular Life Sciences, University of Zurich, Switzerland
* These authors contributed equally to this work.
[2] corresponding author: E-mail: urs.greber@imls.uzh.ch
Telephone: +41 44 635 48 41, Fax: +41 44 635 68 17

Running title:

RV-A16 compensates for low levels of PI4K class 3beta

Abstract (238 w)

Rhinoviruses (RVs) replicate on cytoplasmic membranes derived from the Golgi apparatus. They encode membrane-targeted proteins 2B, 2C and 3A, which control trafficking and lipid composition of the replication membrane. The virus recruits host factors for replication, such as the phosphatidylinositol 4 (PI4)-kinase 3beta (PI4K3b), which boosts PI4-phosphate (PI4P) levels, and drives lipid counter-current exchange of PI4P against cholesterol at endoplasmic reticulum-Golgi membrane contact sites through the lipid shuttling protein oxysterol binding protein (OSBP) 1. We identified a PI4K3b-inhibitor resistant RV-A16 variant with a single point mutation in the conserved 2B protein near the cytosolic carboxy-terminus, isoleucine 92 to threonine [I92T]. The mutation did not confer resistance to cholesterol sequestering compounds or OSBP1 inhibition, suggesting invariant dependency on the PI4P/cholesterol lipid counter-currents. In presence of PI4K3b-inhibitor, Golgi reorganization and PI4P lipid induction occurred in RV-A16 2B[I92], but not wild-type infection. The knock-out of PI4K3b abolished the replication of both 2B[I92T] mutant and wild-type. Doxycyclin-inducible expression of PI4K3b in PI4K3b knock-out cells efficiently rescued the 2B[I92T] mutant, and less effectively wild-type virus infection. Ectopic expression of 2B[I92T] or 2B was less efficient than 3A in recruiting PI4K3b to perinuclear membranes, suggesting a supportive rather than decisive role of 2B in recruiting PI4K3b. The data suggest that 2B tunes the recruitment of PI4K3b to the replication membrane, and allows the virus to adapt to cells with low levels of PI4K3b, yet maintaining the PI4P/cholesterol counter-current for establishing Golgi-derived RV replication membranes.

Importance

Human rhinoviruses (RVs) are the major cause of common cold worldwide. They cause asthmatic exacerbations and chronic obstructive pulmonary disease. Despite recent advances, the development of antivirals and vaccines has proven difficult due to the high number and variability of RV types. The identification of critical host factors and their interactions with viral proteins and membrane lipids for the establishment of viral replication is a basis for drug development strategies. Our findings here shed new light on the interactions between nonstructural viral membrane proteins and class III phosphatidylinositol 4 kinases from the host, and highlight the importance of phosphatidyl-inositol 4 phosphate for RV replication.

Introduction

Human rhinoviruses (RVs) are the most frequent cause of common colds, accounting for about 50% of upper respiratory tract infections (1). Although rarely life threatening, RVs can also replicate in the lower airways where they play a critical role in causing exacerbations of asthma, chronic obstructive pulmonary disease and cystic fibrosis (2). RVs are in the genus *Enterovirus* of the *Picornaviridae* family, and classified into the three species, RV-A, RV-B and RV-C (3). While the recently discovered RV-C types use human cadherin-related family member 3 (CDHR3) as a receptor for entry (4), the major types of the RV-A and B species bind to intercellular adhesion molecule 1 (ICAM1), and the minor types to the low density lipoprotein (LDL) family receptors (5). Receptor binding leads to viral endocytosis and uncoating of the viral RNA genome (6-8).

The replication of plus sense RNA viruses in the cytoplasm occurs in close association with membranes of the secretory or the endocytic pathways (reviewed in 9, 10-12). Picornavirus infections suppress the early onset of apoptosis and execute viral necrosis (13, 14). They remodel cytoplasmic membranes, which involves host protein recruitment to membranes, synthesis and modification of lipids, and alterations in membrane curvature, flux and traffic. RVs remodel cytoplasmic membranes where viral and cellular proteins cooperate to replicate viral RNA, so called replication complexes (15-17). Until recently, the morphology and origin of enterovirus-induced membrane rearrangements remained controversial. Serial electron tomography at different stages of infection revealed that poliovirus (PV) and coxsackievirus (CV) first form convoluted branching membrane tubules, and later on process them into double-membrane vesicles (16, 18). Enterovirus replication complexes are established in close association with *cis*-Golgi membranes, suggesting that Golgi is the initial site of replication complex (RC) formation (19-22). As infection progresses, the Golgi apparatus is disrupted, and replication membrane structures grow in number and complexity in the perinuclear area, near dilated endoplasmic reticulum (ER) tubules.

The membrane-targeted 2B, 2C and 3A proteins have been implicated in remodeling cytoplasmic membranes into replication membranes (23-25). For example, mutations in 2B and 3A facilitated RV-B39 adaptation to virus growth in murine cells expressing the intercellular adhesion molecule 1 (ICAM-1) receptor, and enabled the formation of

replication membranes, thereby highlighting the importance of viral membrane interacting proteins (26).

The formation of the replication membranes also critically depends on host factors, such as phosphatidylinositol 4 (PI4)-kinase class 3b (PI4K3b) (21, 22, 27). In uninfected cells, PI4K3b is located at the Golgi complex through the small GTP-binding protein Arf1 (28). It is activated by phosphorylation at Ser268, and stabilized by interactions with 14-3-3 proteins. Activated PI4K3b catalyzes the formation of PI4-phosphate (PI4P) lipids, which have key roles in signaling and vesicular trafficking at the Golgi complex (29). PI4K3b is recruited to the replication membranes in enterovirus-infected cells, where it generates high levels of PI4P (21, 22). One model for enrichment of PI4K3b at Golgi membranes suggested that the 3A protein of CVB3 indirectly recruits PI4K3b via the PI4K3b effector Arf1, as 3A recruits GBF1 to the replication membranes, activates Arf1 and thus mimics host recruitment mechanisms of PI4K3b (21). Another model proposed that 3A recruits PI4K3b to the replication membranes by direct interactions. Expression of 3A from various enteroviruses, such as PV, CVB3, RV-B14, in absence of other viral proteins showed that 3A co-purified with PI4K3b (30). Interestingly, another host protein, acyl-CoA binding domain containing 3 (ACBD3) also known as GCP60, co-purified with the 3A-PI4K3b complex and was able to bind PI4K3b independently of 3A (30). This suggests that ACBD3 acts as an adaptor for 3A to recruit PI4K3b. Yet, PI4K3b recruitment by CVB3 3A protein can also occur independently of GBF1, Arf1 or ACBD3, suggesting further mechanisms of lipid kinase recruitment to the RCs (31).

Here, we identified a novel mutation in the 2B protein of RV-A16, which was sufficient to render virus resistant to PI4K3b inhibitors or PI4K3b knock-down. The single point mutation occurred in a site, which is highly conserved within species A and B rhinoviruses. Unlike enterovirus 3A mutants, the RV-A16 mutant retained the ability to use the PI4P/cholesterol lipid counter currents on the replication membranes, akin to native RV-A16. The mutant virus could not replicate in absence of PI4K3b but replicated more efficiently at limiting levels of PI4K3b, as shown by dose dependent doxycycline induction of ectopic PI4K3b in PI4K3b knock-oiut (KO) cells. We suggest that the 2B[I92T] mutant protein facilitates the recruitment of PI4K3b to the replication membrane.

Materials and Methods

Chemicals, plasmids, antibodies, and cell lines

PIK93 was purchased from Selleck Chemicals; BFA from LC Laboratories; MbCD, and 25-HC from Sigma; CAY10499 from Cayman Chemical. GSK2998533A (short GSK533A) was a kind gift from from S. You (GlaxoSmithKline, Infectious Disease R&D, North Carolina, USA); compactin from L. Rohrer (Institute of Clinical Chemistry, University Hospital Zurich, Switzerland); AL-9 and C23 from R. De Francesco (Istituto Nazionale di Genetica Molecolare, Milano, Italy). RV-A16 was used as in (32). The RV-A16 genomic replicon pR16 was a gift from W. Lee (Department of Pediatrics, School of Medicine and Public Health, University of Wisconsin, USA). The CVB3 genomic replicons pRLuc-CB3/T7 and pRLuc-CB3/T7-3A[H57Y] were a gift from F. van Kuppeveld (Department of Infectious Diseases & Immunology, University of Utrecht, Netherland). cDNAs encoding the RV-A16 nonstructural proteins myc-2B, myc-3A, myc-3AB were obtained from A. Mousnier (Imperial College London), and expressed from the pRK5-myc plasmid (Clontech) from the CMV promoter and with SV40-poly adenylation signal as described (33). Mouse monoclonal (Mab) 16-7 directed against VP2 (W.M. Lee, Department of Pediatrics, School of Medicine and Public Health, University of Wisconsin, USA) and Mab J2 against dsRNA (English & Scientific Consulting) were used as described (32), rabbit polyclonal antibody against VP1 (from K. Niespodziana and R. Valenta, Division of Immunopathology, University of Graz, Austria, 34), Mabs against GM130 and PI4K3b (BD Transduction Laboratories), Mab against PI4P (Echelon), Mab 1C4 against PI4K2a (S. Minogue, Institute of Liver and Digestive Health, University College London, UK), and Alexa Fluor-488 or -594 labeled secondary antibodies against mouse or rabbit IgG or IgM (Invitrogen). HeLa cervical carcinoma cells strain Ohio (HeLa, from L. Kaiser, Central Laboratory of Virology, University Hospital Geneva, Switzerland) were cultured in Dulbecco's Modified Eagle Medium (DMEM) supplemented with 10% heat-inactivated fetal bovine serum (FBS) and 1% L-glutamine, called full medium.

Generation of PIK93-resistant viruses

HeLa cells were cultured in 96-well plates overnight at 37°C in full medium, and infected with wild-type (WT) RV-A16. PIK93-resistant viruses were obtained by serial passages in presence of increasing concentrations of PIK93 for 6 days at 33.5°C. Supernatants from cultures with full CPE at highest concentration of drug were

passaged until full CPE was observed at a PIK93 concentration that did not allow replication of the initial inoculum (for example, WT virus at 1 μM PIK93). Resistant virus pools were subjected to plaque purification by culturing HeLa cells in 6-well plates at 37°C in full medium overnight, inoculated with the PIK93-resistant virus pool in 10-fold dilution series in full medium complemented with 1 μM PIK93 at 33.5°C. At 5 h post-infection, the medium was discarded and replaced by fresh full medium complemented with 0.6% agarose (Affymetrix), 1% penicillin/streptomycin solution (Gibco), and 1 μM PIK93. The 6-well plates were incubated for 6 days at 33.5°C. Single plaques were identified and collected for further amplification in HeLa cells on 6-well plates for 2 days at 33.5°C. Total RNA was extracted using TRI reagent, and cDNAs obtained by reverse transcription using SuperScript III according to the manufacturer's instructions. PCR fragments covering the nonstructural region of RV-A16 were amplified using Pfu polymerase (Promega) and analyzed by Sanger DNA sequencing.

Site-directed mutagenesis

The site-specific substitution I92T was introduced into the genomic replicon clone of RV-A16 by PCR overlap extension. The first PCR reaction using Pfu polymerase generated two fragments with overlapping ends. The sense primer (5'-AAA GCT TCC TAG GCA GAT CG-3') and the anti-sense primer harboring the I92T mutation (5'-CTG ATT CTT TGT GTG TAT AAG TTA ATT-3') were used to amplify the first fragment with the genomic replicon pR16 as template. The second fragment was generated with the same template, the anti-sense primer (5'-TTC ACT GCC CGG GTC AGC AT-3') and the sense primer harboring the I92T mutation (5'- CAA TTA ACT TAT ACA CAC AAA GAA TCA-3'). The PCR amplification occurred as follows: pre-heating at 94°C for 2 min, denaturation at 94°C for 30 sec, annealing at 55°C for 30 sec, and extension at 72°C for 2 min. The cycle was conducted 25 times, followed by incubation at 72°C for 5 min. The amplified PCR fragments were purified and extracted by electrophoresis from a 1% agarose gel. The second PCR round involved the two overlapping fragments as templates and the two primers located at both ends. The final fragment was amplified with Pfu polymerase as follows: pre-heating at 94°C for 2 min, denaturation at 94°C for 30 sec, annealing at 55°C for 30 sec, and extension at 72°C for 4 min. The cycle was conducted 25 times, followed by incubation at 72°C for 5 min. The final amplified PCR fragment harboring the I92T mutation was gel purified, sequentially digested with AvrII and XmaI restriction

enzymes (Promega), and reintroduced into the original pR16 plasmid. Presence of the mutation in the newly generated genomic replicon pR16 2B[I92T] was confirmed by sequencing.

In vitro RNA transcription and crude virus stock production

The plasmids pR16 WT and pR16 2B[I92T] were linearized with SacI (Promega), extracted with phenol:chloroform, and *in vitro* transcribed using T7 RNA polymerase (Fermentas) according to manufacturer's instructions at 37°C for 2 h, DNAse and RNA treated, and extracted by phenol:chloroform. HeLa cells were cultured in 24-well plates overnight at 37°C in full medium, transfected with 250 ng of purified RNA using the TransIT-mRNA transfection kit (Mirus) according to manufacturer's instructions. When cultures exhibited extensive CPE after 2 days of incubation at 37°C, virus was harvested from cells and supernatant, freeze/thawed three times, and centrifuged at 5000 x g for 5 min. Supernatants were collected, and titrated in a $TCID_{50}$ assay. Equal MOIs from pR16 WT and pR16 2B[I92T] stocks were used in infection assays.

Interference and high-throughput infection

Small interfering RNAs (siRNAs) were reverse transfected to HeLa cells in 96-well plates using serum-free Opti-MEM (Invitrogen) and Lipofectamine RNAiMAX (Invitrogen) (20 nM, 37°C, 72 h), and inoculated with crude virus stocks (MOI 20) at 33.5°C for 8 h. For chemical interference assay, HeLa cells were treated with drugs at 1 h pi, infected with crude virus stocks (MOI 20) at 33.5°C for 8 h, fixed, stained with Mab J2, and scored for infection. Images were acquired with an ImageXpress Micro microscope (Molecular Devices) in automated mode, using a CoolSNAP HQ 12bit gray scale camera (Roper Scientific) and 10x/NA 0.5 objective (Nikon), and analyzed with a custom written script in Matlab (MathWorks, Inc. Natick, MA, USA) (35-37), or in R. Infection indexes were calculated as the fraction of infected cells per total cell number, and plotted with GraphPad Prism software (GraphPad), or with R.

Immunofluorescence and confocal microscopy

HeLa cells on coverslips were treated with PIK93 and infected with crude virus stocks at 33.5°C for 8 h. Alternatively, HeLa cells were transfected with plasmid DNA using Lipofectamine 2000 (Invitrogen) for 24 h. For PI4P staining, plasma membrane and cytoplasmic PI4P pools were stained, and quantitated by expanding the DAPI-mask as described (22, 38). Other immunofluorescence staining was done with cells fixed

with 4% PFA and permeabilized with 0.2% Triton X-100, blocked for 1 h in PBS supplemented with 1% bovine serum albumin (BSA), followed by primary antibodies in blocking buffer overnight at 4°C. Alexa Fluor-488 or -594 secondary antibodies were used in blocking buffer for 1 h. Coverslips were mounted in mounting medium (Dako) and analyzed with an upright Leica TCS SP8 scanning laser confocal microscope with an HCX PL APO 63×/1.4 oil immersion objective. Images were acquired using LAS AF software (Leica), processed with ImageJ (National Institutes of Health), and quantitated as described earlier (22). Quantification of PI4P signal in single cells was carried out by maximal projection of eight z-stacked images of 2 µm width for each channel. An outline extending 10 pixels from the nuclear periphery based on DAPI staining was used to define a perinuclear area for PIP4 intensity quantification. The average score normalized by area was plotted as relative fold change.

CRISPR/Cas9 knock-out and inducible expression of PI4K3b

Knock-out HeLa-OHIO cell lines were generated with a modified version of the lentiCRISPRv2 one vector system described in (39). The Cas9 cassette was exchanged with the high-fidelity Cas9 variant by using the *XbaI* and *BamHI* restriction sites (40). For tetracycline inducibility, the promotor region was extended at the *EcoRI*, *XbaI* and the *XhoI* sites by the thyroid hormone response element (TRE), the TetR on pCW57.1 (Addgene 41393) and the EF1a from Lenti-eCas9 (Addgene 52962). The sequences introduced into the plasmid as templates for the gRNA were 5'-GCACGGCAGTTACACCACTG-3' for the PI4K3b KO, and 5'-GGATCCTGAGTTCGAGGCGG-3' for the PI4K2a KO. Clonal knock-out cell lines were raised by limiting dilution of parental polyclonal cells. Individual clones were analyzed for expression of PI4K2a or PI4K3b by Western blotting.

For the generation of a cell line expressing tetracycline-inducible PI4K3b, full-length complementary DNA (cDNA) of *Homo sapiens* PI4K3b (accession no. XM_005245264.3) was cloned into the lentiviral expression vector pLVX-IRES-Puro (Clontech) using the *XhoI* and the *NotI* restriction sites. Lentiviral particles were produced by co-transfecting HEK-293T cells with pCMVR8.91-Gag-Pol and pVSV-G (Clontech) and the lentiviral expression constructs. HeLa-OHIO or HeLa-OHIO PI4K3b KO cells were transduced with the lentiviral particles and cultured in 5 µg/ml puromycin (Invitrogen). Tetracycline-inducible PI4K3b was expressed by doxycycline at indicated concentrations.

Results

PIK93-resistant RV-A16 is mutated in 2B

PI4K3b is a key host factor for replication of enteroviruses, and chemical inhibitors of PI4K3b block enterovirus infections (12). Mutants of PV, CVB3 and RV-B14 that had been found to be resistant to PI4K3b inhibitors all carried mutations in 3A. However, no RV-A mutants were reported (41-44). RV-A16 is highly sensitive to PIK93, which binds to the ATP binding site of PI4K3b (45). PIK93 has a half effective concentration (EC_{50}) of 250 nM (22). We investigated whether PIK93-resistant mutants would also occur in the 3A protein of RV-A16. RV-A16 was serially cultured in presence of increasing concentrations of PIK93. After 11 passages, a PIK93-selected RV-A16 pool emerged that grew in presence of 1 µM PIK93 (not shown). When this pool of mutants was inoculated to fresh cells at MOI 20 for 8 h, it gave rise to infection in presence of up to 4 µM PIK93, whereas RV-A16 WT was strongly inhibited by low concentrations of PIK93 (Fig. 1A). Inoculation with different amounts of virus at 1 µM PIK93 gave rise to dose-dependent infections, in which the PIK93-selected variant replicated better than the WT at comparable MOI (Fig. 1B). This shows that we selected RV-A16 variants resistant to PIK93.

Viruses from the pool were plaque purified in presence of 1 µM PIK93 and 12 independent clones were picked for genotyping. Sequencing of genomic segments encompassing the nonstructural proteins 2B, 2C, 3A, 3B, 3C, and 3D showed that all 12 clones had a single point mutation in the membrane-associated protein 2B at position isoleucine 92 to threonine [I92T]. With the exception of a silent mutation in the 3C protein, no other mutations were observed. 2B is a small protein of about 100 amino acids and contains two hydrophobic domains required for membrane binding and correct localization in ER and Golgi membranes (46). The [I92T] mutation in the cytoplasmic C-terminal tail of 2B is located in a highly conserved region, indicated by amino acid sequence alignment of 99 RV-A and RV-B types (Fig. 1C, D). The [I92T] mutation facing the cytosol alters the side chain properties from a hydrophobic (I) to a polar (T) amino acid, and could be in direct contact with a host or viral protein to compensate for the reduction in PI4P.

The 2B[I92T] mutant is resistant to PI4K3b inhibitors and depends on OSBP1

To test if the [I92T] mutation in 2B was necessary and sufficient to confer resistance to PI4K3b inhibitors, we introduced the 2B[I92T] mutation to a plasmid encoding an infectious full-length RV-A16 WT genome (pR16.11), and generated crude virus stocks from RV-A16 WT and RV-A16 2B[I92T] replicons. The PI4K3b inhibitors PIK93 and GSK533A reduce RV-A16 replication at EC_{50} of 250 nM and 40 nM, respectively (22). Both compounds were less effective against RV-A16 2B[I92T], as indicated by immunofluorescence infection assays using anti-dsRNA antibodies (Fig. 2A). Notably, the Arf-GEF inhibitor brefeldin A (BFA) was similarly effective against both WT and 2B[I92T], validating the assay system used here. The calculated EC_{50} of PIK93 for RV-A16 2B[I92T] was 1.8 µM, about 3 fold higher compared to RV-A16 WT, which was previously shown to be 0.6 µM (22). Similarly, the 2B[I92T] mutant replicated better than RV-A16 WT in the presence of GSK533A with 2.3 fold higher EC_{50} than WT (73.9 nM and 32.5 nM, respectively). The reduced sensitivity of RV-A16 2B[I92T] to PIK93 and GS533A was in the same range as for a PI4K3b resistant CVB3 mutant 3A[H57Y], reported earlier (44), which was as sensitive to BFA as native CVB3 (Fig. 2B). The data show that the 2B[I92T] mutation conferred resistance to PI4K3b inhibitors independent of the chemical mode of inhibition, suggesting a role of the 2B protein in the recruitment or activation of PI4K3b for RV-A16 replication.

In addition to PI4K3b, enterovirus replication critically depends on PI4P/cholesterol counter-currents at the replication membranes, and the lipid exchange protein OSBP1 (22, 47, 48). The RV-A16 2B[I92T] mutant was as dependent on OSBP1 and cholesterol as native RV-A16, indicated by sensitivity to the OSBP1 inhibitor 25-hydroxycholesterol (25-HC), and the cholesterol esterase inhibitor CAY10499, with EC_{50} values of 0.86 µM, 2.16 µM for RV-A16 2B[I92T], and 0.97 µM, 2.62 µM for RV-A16 WT, respectively (Fig. 3A, B). 25-HC binds to the cholesterol binding pocket of OSBP1 with higher affinity than cholesterol, and blocks the lipid exchange activity of OSBP1 (49). This contrasts the CVB3 3A[H57Y] mutant, which was insensitive to both the 25-HC and CAY10499, unlike CVB3 WT, which was sensitive to high concentrations of 25-HC (Fig. 3C, D). The dependency of RV-A16 2B[I92T] on cholesterol was further supported by the finding that it was at least as sensitive to the cholesterol sequestering compound methyl-β-cyclodextrin (MbCD) as RV-A16, with

EC_{50} values of 2.16 μM, and 2.62 μM, respectively (Fig. 3E). Both RVs were insensitive to the cholesterol synthesis inhibitor compactin (Fig. 3F) (50), as reported earlier for RV-A16 (22). The data thus far show that RV-A16 2B[I92T] depends on cholesterol, cholesterol esterases and the PI4P/cholesterol exchange protein OSBP1.

The RV-A16 2B[I92T] mutant requires other PI4Ks than PI4K3b

To further explore how the 2B[I92T] mutant uses the PI4P/cholesterol lipid counter currents, we transfected cells by siRNA targeting OSBP1 and PI4K3b, inoculated virus at MOI 20, and analyzed infections by immunofluorescence against dsRNA and high throughput-automated microscopy. As expected, RV-A16 2B[I92T] was nearly as sensitive to OSBP1 knock-down as RV-A16 WT, and much less sensitive to PI4K3b knock-down (Fig. 4A). This suggested that the virus can take advantage of PI4K3b if this enzyme is available. The selective PI4K3a inhibitor C23 neither inhibited RV-A16 WT nor RV-A16 2B[I92T] (Fig. 4B). C23 is 100-fold more selective against PI4K3a than PI4K3b, with IC_{50} values of 16 nM and 1.6 μM, respectively (51), which makes it unlikely that PI4K3a is used for RV-A16 2B[I92T] infection.

RV-A16 2B[I92T] disperses the Golgi apparatus in presence of PIK93

To further analyze how 2B[I92T] replicates and drives the PI4P/cholesterol counter-current we investigated the integrity of the cis-Golgi by GM130 staining. As expected from previous results with RV-A16 (22), both RV-A16 WT and 2B[I92T] infections lead to dispersion of the Golgi apparatus in absence of PIK93 (Fig. 5). RV-A16 2B[I92T] but not WT dispersed the Golgi membrane in presence of PIK93 (Fig. 5). 2B[I92T] infection increased the overall cytoplasmic levels of PI4P even in presence of PIK93, indicated by anti-PI4P antibody staining (Fig. 6A). In the absence of PIK93, the perinuclear PI4P levels significantly increased 2.8 and 2.67-fold in RV-A16 WT and 2B[I92T] infected cells, respectively, and 2.3-fold in 2B[I92T] infected cells in presence of PIK93 (Fig. 6B). PIK93 strongly blocked perinuclear PI4P increase in WT infected cells.

To explore if class III PI4Ks were involved in the increase of PI4P in 2B[I92T] infected cells, we immuno-stained cells with antibodies against PI4K3b. Infected cells were scored by antibodies against the capsid proteins VP1. PI4K3b was enhanced in the perinuclear area by both WT and 2B[I92T] virus infections (Fig. 6C, D). In control cells, the recruitment of PI4K3b was higher in cells infected with the 2B[I92T] mutant

than WT, that is 2.44 and 1.86-fold respectively. PIK93 significantly abrogated the enrichment of PI4K3b to perinuclear areas of WT, but not 2B[I92T] mutant infected cells, where the perinuclear levels were 2.11-fold higher than in uninfected cells. This suggests that the 2B[I92T] mutation enhances the recruitment of PI4K3b at the replication membranes, even in presence of PIK93.

RV-A16 2B[I92T] replicates at low levels of PI4K3b

To scrutinize if the 2B[I92T] mutant takes advantage of very low levels of PI4K3b, we engineered a cell line for doxycycline (Dox)-inducible expression of PI4K3b in the background of PI4K3b KO HeLa-OHIO cells. The PI4K3b knock-out (KO) cells were completely resistant to WT and the 2B[I92T] mutant virus, while PI4K2a KO cells were fully susceptible to both viruses (Fig. 7A). Dox induced PI4K3b in a dose dependent manner (Fig. 7B). Notably, the induced PI4K3b was running slightly faster in the SDS-PAGE than the endogenous HeLa cell protein. The cDNA encoding the induced PI4K3b was missing the exon encoding amino acids 304 – 318 accounting for about 1.5 kDa. Since the difference between the endogenous and the induced PI4K3b is about 10 kDa, and a faint upper band running at the position of the endogenous protein is present in the induced cells, we suspect that the two bands differ in the levels of post-translational modifications, such as sumoylation, phosphorylation or ubiquitination. Regardless, the expression of PI4K3b enhanced the titers of WT by 1.67 logs, and the 2B[I92T] mutant by 2.33 logs (Fig. 7C). The enhancement of infection was consistently larger for the 2B[I92T] mutant than the WT, as indicated by measuring VP2 production at different dosage of Dox at both 8 and 16 h pi (Fig. 7D). These results indicate that the 2B[I92T] mutant replicates better at low PI4K3b levels than WT.

The RV-A16 3A protein recruits PI4K3b

We examined if one of the nonstructural viral proteins recruits the kinase responsible for PI4P generation. HeLa cells were transfected with myc-tagged viral protein 2B WT, 2B[I92T], 3A or 3AB, and analyzed by immuno-fluorescence staining against PI4P, and PI4K3b. None of the viral proteins except 3AB enhanced the levels of PI4P (Fig. 8A), in agreement with results from other enteroviruses (48). Expression of 3A protein was sufficient to recruit PI4K3b at perinuclear sites, while 3AB was less efficient in doing so (Fig. 8B). Notably, neither 2B WT nor 2B[I92T] proteins had an apparent effect on intracellular PI4P levels or PI4K3b recruitment. This suggests that

the 3A protein is the predominant recruitment factor for PI4K3b to perinuclear membranes, and the 3AB precursor an enhancer of PI4P levels, perhaps by activating PI4K activity. In sum, RV-A16 2B[I92T] alone is not able to enhance PI4P levels or to recruit PI4K3b to perinuclear membranes. This excludes the 2B protein as a stand-alone recruiting factor for PI4K3b, but rather suggests a supporting or stabilizing role of 2B in the recruitment of PI4K3b by 3A and 3AB.

Discussion

The best studied picornaviruses are enteroviruses. Enteroviruses comprise 12 genera *Enterovirus* A-J and *Rhinovirus* A, B, C, and include well known agents, such as PV, coxsackieviruses and human rhinoviruses. These viruses all induce the formation of single membrane clusters in proximity to Golgi and ER within just a few hours of infection. The replication membranes grow in size, complexity and volume as infection progresses, and eventually become double membrane structures. In case of PV and members of the alphavirus-like superfamily, such as bromovirus, this involves changes in fatty acid metabolism, fatty acid import and phospholipid synthesis, including phosphatidyl choline (PC) (52, 53). Another key lipid for enterovirus replication membranes is cholesterol. While *de novo* cholesterol synthesis is not required, exogenous cholesterol from receptor-mediated endocytosis or de-esterification of cholesterol-esters from lipid droplets is essential for enterovirus replication (for review, see 12). Free cholesterol is delivered to the replication membrane by OSBP1 and related proteins at membrane contact sites (22, 54, 55). This occurs by a lipid counter current flux exchanging PI4P and cholesterol, and is driven by the formation of PI4P through PI4Ks (28, 56). For replication of enteroviruses, including PV, CVB3, and RV-A and -B, the Golgi-associated PI4K3b is of key importance, although RV-A1A and A16 can also use PI4K2a and PI4K3a, as suggested by RNA interference (21, 22, 57). Notably, however, the Clustered Regularly Interspaced Short Palindromic Repeats (CRISPR)/Cas9 mediated KO of PI4K2a had no effects on RV-A16 infection (see Fig. 7A). These data highlight the complexity of virus-tuned lipid modulation.

How PI4Ks are recruited to replication membranes is poorly understood. For enteroviruses, it was initially suggested that PI4K3b is recruited by 3A protein, either indirectly via GBF1 and Arf1, or directly using ACDB3 as an adaptor (reviewed in 58).

Yet, none of these options proved to be conclusive. Instead, the expression of CVB3 3A protein alone was sufficient to recruit PI4K3b and generate high level of PI4P lipids, even in GBF1, Arf1 or ACDB3 depleted cells (21, 31). A recent study suggested that the CVB3 mutant 3A[H57Y] can replicate in presence of PI4K3b inhibitors and without apparent dedicated replication membranes on Golgi membranes (59). Based on our results we speculate that this mutant grows in presence of low concentrations of active PI4K3b, perhaps akin to the 2B[I92T] mutant.

We show that the 2B[I92T] mutant confers resistance to PI4K3b inhibitors. Isoleucine 92 is highly conserved among RV-A and RV-B species and located near the cytosolic carboxy-terminus of 2B. 2B comprises about 100 amino acids, forms membrane pores by virtue of two hydrophobic domains and oligomerization, localizes to Golgi membranes, and inhibits protein trafficking (46, 60, 61). Similar to 3A, expression of RV-A16 2B protein alone suffices to block protein secretion, although RV-A16 infection did not apparently inhibit the release of a reporter protein Gaussia luciferase up to 7 h pi, suggesting that virus infection does not block the entire secretory pathway (33).

Remarkably, the RV-A16 2B[I92T] disrupted the Golgi, recruited PI4K3b, and enriched PI4P on replication membranes in the presence of PI4K3b inhibitors. RV-A16 2B[I92T] remained sensitive to other inhibitors of the PI4P/cholesterol counter-current flux. Remarkably, PI4K3b localizes close to OSBP1, and thereby allows the steady exchange of lipids between the ER and the Golgi stacks, depending on the OSPB1 anchoring protein VAP (62). VAP was also important for RV replication, as shown by RNA interference and the expression of dominant-negative OSPB1 mutants lacking the PI4P binding domain but retaining the VAP binding domain FFAT (22). PI4K2a which does not locate to the proximity of OSBP1 leads to oscillating flux of PI4P (62), and this correlates with PI4K2a being unable to support RV-A16 replication (see Fig. 7A).

The phenotype of RV-A16 2B[I92T] appears to be different from the previously reported 3A mutants, which to replicate in a PI4K3b-independent manner when PI4K3b activity is impaired (41-44). This suggests that the A16 2B protein has a different function(s) than 3A protein in the generation of replication membranes. In support of this notion, the expression of 3A but not 2B protein alone recruited PI4K3b, and the precursor 3AB increased PI4P levels in transfected cells. This is

different from the coxsackievirus (CV) 3A protein, which recruited PI4K3b and increased PI4P (44). Further, the replication of the CVB3 3A[H57Y] mutant in presence of PI4K inhibitors no longer depended on PI4K3b, or other PI4K isoforms, did not disrupt the Golgi membranes, and did not increase the PI4P levels (44).

In contrast, the RV-A16 2B[I92T] mutant replicated at lower levels of PI4K3b than WT, as indicated by tunable expression of PI4K3b, and two different chemicals targeting the ATP binding site of PI4K3b. It was sensitive to RNA interference against PI4K3b, suggesting either a lower requirement, or a non-enzymatic function of PI4K3b for RV-A16 2B[I92T] replication. Notably, PI4K3b recruits small GTPases independent of its catalytic activity, and fine tunes vesicular transport (45). Consistently, the complete knock-out of PI4K3b by CRISPR/Cas9 abrogated both RV-A16 WT and 2B[I92T] infections, which were however insensitive to PI4K2a knock-out. This strengthens the notion, that the 2B[I92T] reduces, but does not eliminate the requirement for PI4K3b. Low residual functionality of PI4K3b resulting from incomplete inhibition by a compound, or siRNA knockdown would therefore be sufficient for the replication of RV-A16 2B[I92T], but not WT.

It is possible that the transmembrane domains of 2B and 3A or 3AB interact, as suggested for the poliovirus proteins by yeast-two-hybrid experiments (63). We speculate that the respiratory RV-A16 uses the 2B protein together with 3A to recruit PI4K3b. This is based on the notion that there are no RV-A types known to have mutations in 3A, which would make them resistant to PI4K3b inhibitors. Since the N-terminus of 3A from RV-A types lacks 6 amino acids, which are present in RV-B types, we conjecture that RV-A types require an additional viral protein for effective recruitment of PI4Ks to the replication membrane. We further suggest that CVB or RV-B can drive the lipid currents that are crucial for establishing the replication membrane by taking advantage of another asymmetry than PI4P lipids. Such asymmetrically distributed lipids could comprise PC. Notably, the phosphatidyl inositol transfer protein b (PITPb) shuttles phosphatidyl inositol (PI) in exchange to PC between the ER and Golgi membranes, and is required for RV-A1A and RV-A16 replication (22). Intriguingly, PC with short acyl chain lengths are enriched in PV infected cells (52), giving rise to the possibility that PC lipids are involved in tuning the composition of the replication membrane.

In summary, our results show that despite the great plasticity of the host lipid landscape and the readily mutating nonstructural proteins of picornaviruses the cells

provides key metabolic circuits for establishing picornavirus replication membranes. One of these circuits is the PI4P/cholesterol counter-current flux. Host components that regulate this flux are surgically targeted by at least two nonstructural membrane proteins of RV-A16, 2B and 3A to drive viral replication on cytoplasmic membranes.

Acknowledgements

We thank D. Seiler and M. Suomalainen for comments to the manuscript, and the following colleagues for kindly providing reagents: R. De Francesco and P. Neddermann for AL-9 and C23, L. Rohrer for compactin, K. Niespodziana and R. Valenta for antibody against VP1, S. Minogue for Mab 1C4 against PI4K2a, A. Mousnier for cDNAs encoding myc-tagged RV-A16 2B, 3A, 3AB, F. van Kuppeveld for CVB3 genomic replicons, W.M. Lee for Mab 16-7 directed against VP2, and L. Kaiser for HeLa cervical carcinoma cells strain OHIO.

Funding information

This work was supported by the Swiss National Science Foundation (grant number 310030B_160316), a Medical Research and Development Project from the Swiss initiative for systems biology SystemsX.ch (2014/264 Project VirX, evaluated by the Swiss National Science Foundation), and the University of Zurich Research Priority Program ‘Evolution in Action’ to UFG.

Author contributions

U.F.G. conceived and coordinated study, P.S.R. and L.P.M. performed experiments, P.S.R., L.P.M. and U.F.G. interpreted results, and wrote the manuscript.

References

1. **Makela MJ, Puhakka T, Ruuskanen O, Leinonen M, Saikku P, Kimpimaki M, Blomqvist S, Hyypia T, Arstila P.** 1998. Viruses and bacteria in the etiology of the common cold. J Clin Microbiol **36:**539-542.

2. **Gern JE.** 2010. The ABCs of rhinoviruses, wheezing, and asthma. J Virol **84:**7418-7426.
3. **McIntyre CL, Savolainen-Kopra C, Hovi T, Simmonds P.** 2013. Recombination in the evolution of human rhinovirus genomes. Archives of virology **158:**1497–1515.
4. **Bochkov YA, Watters K, Ashraf S, Griggs TF, Devries MK, Jackson DJ, Palmenberg AC, Gern JE.** 2015. Cadherin-related family member 3, a childhood asthma susceptibility gene product, mediates rhinovirus C binding and replication. Proc Natl Acad Sci U S A **112:**5485-5490.
5. **Uncapher CR, DeWitt CM, Colonno RJ.** 1991. The major and minor group receptor families contain all but one human rhinovirus serotype. Virology **180:**814-817.
6. **Suomalainen M, Greber UF.** 2013. Uncoating of non-enveloped viruses. Curr Opin Virol **3:**27-33.
7. **Blaas D.** 2016. Viral entry pathways: the example of common cold viruses. Wien Med Wochenschr **166:**211-226.
8. **Yamauchi Y, Greber UF.** 2016. Principles of Virus Uncoating: Cues and the Snooker Ball. Traffic **17:**569-592.
9. **den Boon JA, Ahlquist P.** 2010. Organelle-like membrane compartmentalization of positive-strand RNA virus replication factories. Annu Rev Microbiol **64:**241-256.
10. **Konan KV, Sanchez-Felipe L.** 2014. Lipids and RNA virus replication. Curr Opin Virol **9:**45-52.
11. **Harak C, Lohmann V.** 2015. Ultrastructure of the replication sites of positive-strand RNA viruses. Virology **479-480:**418-433.
12. **Belov GA.** 2016. Dynamic lipid landscape of picornavirus replication organelles. Curr Opin Virol **19:**1-6.
13. **Lotzerich M, Roulin PS, Boucke K, Witte R, Georgiev O, Greber UF.** 2018. Rhinovirus 3C protease suppresses apoptosis and triggers caspase-independent cell death. Cell Death Dis **9:**272.
14. **Croft SN, Walker EJ, Ghildyal R.** 2018. Human Rhinovirus 3C protease cleaves RIPK1, concurrent with caspase 8 activation. Sci Rep **8:**1569.
15. **Miller S, Krijnse-Locker J.** 2008. Modification of intracellular membrane structures for virus replication. Nat Rev Microbiol **6:**363-374.
16. **Belov GA, van Kuppeveld FJ.** 2012. (+)RNA viruses rewire cellular pathways to build replication organelles. Curr Opin Virol **2:**740-747.
17. **Belov GA, Sztul E.** 2014. Rewiring of cellular membrane homeostasis by picornaviruses. J Virol **88:**9478-9489.
18. **Limpens RW, van der Schaar HM, Kumar D, Koster AJ, Snijder EJ, van Kuppeveld FJ, Barcena M.** 2011. The transformation of enterovirus replication structures: a three-dimensional study of single- and double-membrane compartments. MBio **2:**e00166-00111.
19. **Belov GA, Nair V, Hansen BT, Hoyt FH, Fischer ER, Ehrenfeld E.** 2012. Complex dynamic development of poliovirus membranous replication complexes. J Virol **86:**302-312.
20. **Bienz K, Egger D, Pasamontes L.** 1987. Association of polioviral proteins of the P2 genomic region with the viral replication complex and virus-induced membrane synthesis as visualized by electron microscopic immunocytochemistry and autoradiography. Virology **160:**220-226.
21. **Hsu NY, Ilnytska O, Belov G, Santiana M, Chen YH, Takvorian PM, Pau C, van der Schaar H, Kaushik-Basu N, Balla T, Cameron CE, Ehrenfeld E, van Kuppeveld FJ, Altan-Bonnet N.** 2010. Viral reorganization of the

secretory pathway generates distinct organelles for RNA replication. Cell **141:**799-811.

22. **Roulin PS, Lotzerich M, Torta F, Tanner LB, van Kuppeveld FJ, Wenk MR, Greber UF.** 2014. Rhinovirus Uses a Phosphatidylinositol 4-Phosphate/Cholesterol Counter-Current for the Formation of Replication Compartments at the ER-Golgi Interface. Cell Host Microbe **16:**677-690.
23. **Cho MW, Teterina N, Egger D, Bienz K, Ehrenfeld E.** 1994. Membrane rearrangement and vesicle induction by recombinant poliovirus 2C and 2BC in human cells. Virology **202:**129-145.
24. **Doedens JR, Giddings TH, Jr., Kirkegaard K.** 1997. Inhibition of endoplasmic reticulum-to-Golgi traffic by poliovirus protein 3A: genetic and ultrastructural analysis. J Virol **71:**9054-9064.
25. **Suhy DA, Giddings TH, Jr., Kirkegaard K.** 2000. Remodeling the endoplasmic reticulum by poliovirus infection and by individual viral proteins: an autophagy-like origin for virus-induced vesicles. J Virol **74:**8953-8965.
26. **Harris JR, Racaniello VR.** 2005. Amino acid changes in proteins 2B and 3A mediate rhinovirus type 39 growth in mouse cells. J Virol **79:**5363-5373.
27. **Spickler C, Lippens J, Laberge MK, Desmeules S, Bellavance E, Garneau M, Guo T, Hucke O, Leyssen P, Neyts J, Vaillancourt FH, Decor A, O'Meara J, Franti M, Gauthier A.** 2013. Phosphatidylinositol 4-kinase III beta is essential for replication of human rhinovirus and its inhibition causes a lethal phenotype in vivo. Antimicrob Agents Chemother **57:**3358-3368.
28. **Balla T.** 2013. Phosphoinositides: tiny lipids with giant impact on cell regulation. Physiol Rev **93:**1019-1137.
29. **D'Angelo G, Vicinanza M, Di Campli A, De Matteis MA.** 2008. The multiple roles of PtdIns(4)P -- not just the precursor of PtdIns(4,5)P2. J Cell Sci **121:**1955-1963.
30. **Greninger AL, Knudsen GM, Betegon M, Burlingame AL, Derisi JL.** 2012. The 3A protein from multiple picornaviruses utilizes the golgi adaptor protein ACBD3 to recruit PI4KIIIbeta. J Virol **86:**3605-3616.
31. **Dorobantu CM, van der Schaar HM, Ford LA, Strating JR, Ulferts R, Fang Y, Belov G, van Kuppeveld FJ.** 2014. Recruitment of PI4KIIIbeta to coxsackievirus B3 replication organelles is independent of ACBD3, GBF1, and Arf1. J Virol **88:**2725-2736.
32. **Jurgeit A, Moese S, Roulin P, Dorsch A, Lotzerich M, Lee WM, Greber UF.** 2010. An RNA replication-center assay for high content image-based quantifications of human rhinovirus and coxsackievirus infections. Virol J **7:**264.
33. **Mousnier A, Swieboda D, Pinto A, Guedan A, Rogers AV, Walton R, Johnston SL, Solari R.** 2014. Human Rhinovirus 16 Causes Golgi Apparatus Fragmentation without Blocking Protein Secretion. J Virol **88:**11671-11685.
34. **Niespodziana K, Napora K, Cabauatan C, Focke-Tejkl M, Keller W, Niederberger V, Tsolia M, Christodoulou I, Papadopoulos NG, Valenta R.** 2012. Misdirected antibody responses against an N-terminal epitope on human rhinovirus VP1 as explanation for recurrent RV infections. Faseb J **26:**1001-1008.
35. **Jurgeit A, McDowell R, Moese S, Meldrum E, Schwendener R, Greber UF.** 2012. Niclosamide is a proton carrier and targets acidic endosomes with broad antiviral effects. PLoS Pathog **8:**e1002976; 1002910.1001371/journal.ppat.1002976.
36. **Yakimovich A, Andriasyan V, Witte R, Wang IH, Prasad V, Suomalainen M, Greber UF.** 2015. Plaque2.0-A High-Throughput Analysis Framework to

Score Virus-Cell Transmission and Clonal Cell Expansion. PLoS One **10:**e0138760.
37. **Yakimovich A, Yakimovich Y, Schmid M, Mercer J, Sbalzarini IF, Greber UF.** 2016. Infectio: a Generic Framework for Computational Simulation of Virus Transmission between Cells. mSphere **1**.
38. **Hammond GR, Schiavo G, Irvine RF.** 2009. Immunocytochemical techniques reveal multiple, distinct cellular pools of PtdIns4P and PtdIns(4,5)P(2). Biochem J **422:**23-35.
39. **Sanjana NE, Shalem O, Zhang F.** 2014. Improved vectors and genome-wide libraries for CRISPR screening. Nat Methods **11:**783-784.
40. **Slaymaker IM, Gao L, Zetsche B, Scott DA, Yan WX, Zhang F.** 2016. Rationally engineered Cas9 nucleases with improved specificity. Science **351:**84-88.
41. **Heinz BA, Vance LM.** 1995. The antiviral compound enviroxime targets the 3A coding region of rhinovirus and poliovirus. J Virol **69:**4189-4197.
42. **Brown-Augsburger P, Vance LM, Malcolm SK, Hsiung H, Smith DP, Heinz BA.** 1999. Evidence that enviroxime targets multiple components of the rhinovirus 14 replication complex. Arch Virol **144:**1569-1585.
43. **De Palma AM, Thibaut HJ, van der Linden L, Lanke K, Heggermont W, Ireland S, Andrews R, Arimilli M, Al-Tel TH, De Clercq E, van Kuppeveld F, Neyts J.** 2009. Mutations in the nonstructural protein 3A confer resistance to the novel enterovirus replication inhibitor TTP-8307. Antimicrob Agents Chemother **53:**1850-1857.
44. **van der Schaar HM, van der Linden L, Lanke KH, Strating JR, Purstinger G, de Vries E, de Haan CA, Neyts J, van Kuppeveld FJ.** 2012. Coxsackievirus mutants that can bypass host factor PI4KIIIbeta and the need for high levels of PI4P lipids for replication. Cell Research doi:10.1038/cr.2012.129.
45. **Burke JE, Inglis AJ, Perisic O, Masson GR, McLaughlin SH, Rutaganira F, Shokat KM, Williams RL.** 2014. Structures of PI4KIIIbeta complexes show simultaneous recruitment of Rab11 and its effectors. Science **344:**1035-1038.
46. **de Jong AS, de Mattia F, Van Dommelen MM, Lanke K, Melchers WJ, Willems PH, van Kuppeveld FJ.** 2008. Functional analysis of picornavirus 2B proteins: effects on calcium homeostasis and intracellular protein trafficking. J Virol **82:**3782-3790.
47. **Albulescu L, Strating JR, Wubbolts R, van Kuppeveld FJ.** 2015. Cholesterol shuttling is important for RNA replication of coxsackievirus B3 and encephalomyocarditis virus. Cell Microbiol doi:10.1111/cmi.12425.
48. **Dorobantu CM, Albulescu L, Harak C, Feng Q, van Kampen M, Strating JR, Gorbalenya AE, Lohmann V, van der Schaar HM, van Kuppeveld FJ.** 2015. Modulation of the Host Lipid Landscape to Promote RNA Virus Replication: The Picornavirus Encephalomyocarditis Virus Converges on the Pathway Used by Hepatitis C Virus. PLoS Pathog **11:**e1005185.
49. **Wang PY, Weng J, Lee S, Anderson RG.** 2008. The N terminus controls sterol binding while the C terminus regulates the scaffolding function of OSBP. J Biol Chem **283:**8034-8045.
50. **Endo A, Kuroda M, Tsujita Y.** 1976. ML-236A, ML-236B, and ML-236C, new inhibitors of cholesterogenesis produced by Penicillium citrinium. J Antibiot (Tokyo) **29:**1346-1348.
51. **Leivers AL, Tallant M, Shotwell JB, Dickerson S, Leivers MR, McDonald OB, Gobel J, Creech KL, Strum SL, Mathis A, Rogers S, Moore CB, Botyanszki J.** 2014. Discovery of selective small molecule type III

phosphatidylinositol 4-kinase alpha (PI4KIIIalpha) inhibitors as anti hepatitis C (HCV) agents. J Med Chem **57:**2091-2106.

52. **Nchoutmboube JA, Viktorova EG, Scott AJ, Ford LA, Pei Z, Watkins PA, Ernst RK, Belov GA.** 2013. Increased long chain acyl-Coa synthetase activity and fatty acid import is linked to membrane synthesis for development of picornavirus replication organelles. PLoS Pathog **9:**e1003401.
53. **Zhang J, Zhang Z, Chukkapalli V, Nchoutmboube JA, Li J, Randall G, Belov GA, Wang X.** 2016. Positive-strand RNA viruses stimulate host phosphatidylcholine synthesis at viral replication sites. Proc Natl Acad Sci U S A **113:**E1064-1073.
54. **Mesmin B, Bigay J, Moser von Filseck J, Lacas-Gervais S, Drin G, Antonny B.** 2013. A four-step cycle driven by PI(4)P hydrolysis directs sterol/PI(4)P exchange by the ER-Golgi tether OSBP. Cell **155:**830-843.
55. **Strating JR, van der Linden L, Albulescu L, Bigay J, Arita M, Delang L, Leyssen P, van der Schaar HM, Lanke KH, Thibaut HJ, Ulferts R, Drin G, Schlinck N, Wubbolts RW, Sever N, Head SA, Liu JO, Beachy PA, De Matteis MA, Shair MD, Olkkonen VM, Neyts J, van Kuppeveld FJ.** 2015. Itraconazole Inhibits Enterovirus Replication by Targeting the Oxysterol-Binding Protein. Cell Rep doi:10.1016/j.celrep.2014.12.054.
56. **De Matteis MA, Wilson C, D'Angelo G.** 2013. Phosphatidylinositol-4-phosphate: the Golgi and beyond. Bioessays **35:**612-622.
57. **Arita M.** 2014. Phosphatidylinositol-4 kinase III beta and oxysterol-binding protein accumulate unesterified cholesterol on poliovirus-induced membrane structure. Microbiol Immunol doi:10.1111/1348-0421.12144.
58. **van der Schaar HM, Dorobantu CM, Albulescu L, Strating JR, van Kuppeveld FJ.** 2016. Fat(al) attraction: Picornaviruses Usurp Lipid Transfer at Membrane Contact Sites to Create Replication Organelles. Trends Microbiol doi:10.1016/j.tim.2016.02.017.
59. **Melia CE, van der Schaar HM, Lyoo H, Limpens R, Feng Q, Wahedi M, Overheul GJ, van Rij RP, Snijder EJ, Koster AJ, Barcena M, van Kuppeveld FJM.** 2017. Escaping Host Factor PI4KB Inhibition: Enterovirus Genomic RNA Replication in the Absence of Replication Organelles. Cell Rep **21:**587-599.
60. **Doedens JR, Kirkegaard K.** 1995. Inhibition of cellular protein secretion by poliovirus proteins 2B and 3A. EMBO J **14:**894-907.
61. **Cornell CT, Kiosses WB, Harkins S, Whitton JL.** 2006. Inhibition of protein trafficking by coxsackievirus b3: multiple viral proteins target a single organelle. J Virol **80:**6637-6647.
62. **Magdeleine M, Gautier R, Gounon P, Barelli H, Vanni S, Antonny B.** 2016. A filter at the entrance of the Golgi that selects vesicles according to size and bulk lipid composition. Elife **5**.
63. **Yin J, Liu Y, Wimmer E, Paul AV.** 2007. Complete protein linkage map between the P2 and P3 non-structural proteins of poliovirus. J Gen Virol **88:**2259-2267.

Figure Legends

FIG 1: Identification of a PIK93-resistant RV-A16 2B[I92T] mutant

(**A**) HeLa cells were infected with RV-A16 WT (white bars) or RV-A16 PIK93-resistant virus pool (black bars) at a MOI 20 for 8 h. Cells were treated with PIK93 at indicated concentrations, and infection efficiencies were analyzed by high-throughput immunofluorescence microscopy using anti-VP2 antibodies. The ratio of infected cells was calculated and normalized to control infection without drug. Values represent the means ± SD, n=2.

(**B**) HeLa cells were infected with RV-A16 WT (white bars) or RV-A16 PIK93-resistant pool (black bars) at indicated MOI for 8 h, in presence of 1 µM PIK93. Experiment was analyzed as in panel A. Values represent means ± SD, n=2.

(**C**) Pairwise alignment of 2B proteins from RV-A1 (formerly known as RV-A1a or RV-A1b), -A2, -A16, -B14, and -B37, and CVB3 by ClustalW using a Blosum62 similarity matrix. The hydrophobic regions 1 and 2 are present in all proteins and separated by a five amino acid spacer. Note that the isoleucine located at the 92 position (I92) is near the C-terminal end.

(**D**) ClustalW alignement of 2B amino acid sequences from 99 different RV types (74 RV-A and 25 RV-B; 11 minor RV and 88 major RV) using a Blosum62 similarity matrix. Prevalence of the amino acids isoleucine (I) and valine (V) at position 92 or equivalent were depicted by WebLogo from the aligned sequences. In addition, the prevalence of the amino acid threonine (T) at position 92 or equivalent was depicted for the 12 clones selected in the PIK93-selected mutant pool.

FIG 2: Resistance of the RV-A16 2B[I92T] mutant to PI4K3b inhibitors

(**A**) HeLa cells were infected with RV-A16 WT (white bars) or RV-A16 2B[I92T] (black bars) at a MOI of 20 for 8h, in presence or absence or brefeldin A (BFA), PIK93 or GSK533A. Data were analyzed as described in Fig. 1, except that anti-dsRNA staining was used here, and normalized to the DMSO control. Values represent means ± SD, n=2.

(**B**) Same experiment as in panel (A), except that cells were infected with CVB3 WT (white bars) or CVB3 3A[H57Y] (black bars).

FIG 3: Similar susceptibility of RV-A16 2B[I92T] and WT to inhibitors blocking PI4P/cholesterol counter-currents

HeLa cells were infected with RV-A16 WT (white bars) or RV-A16 2B[I92T] (black bars) at a MOI of 20 for 8 h (**panels A, B, E, F**), or with CVB3 WT or the 3A[H57Y] mutant (**C, D**), in presence or absence of brefeldin A (BFA), the OSBP inhibitor 25-HC (**A, C**), the cholesterol esterase inhibitor CAY10499 (**B, D**), the cholesterol depleting drug MbCD (**E**), or the cholesterol synthesis inhibitor compactin (**F**). Infections were analyzed as described in figure 1. Values represent means ± SD, n=2.

FIG 4: Dependency of RV-A16 2B[I92T] on PI4Ks

(**A**) HeLa cells were transfected with siRNA against OSBP1, PI4K3b, or the negative control siRNA (all star, Qiagen). Three days post-transfection, cells were infected with RV-A16 WT (white bars) or RV-A16 2B[I92T] (black bars) at a MOI 20 for 8 h, and analyzed for fraction of infected cells. Values represent means ± SD, n=2. Western blots against OSBP1 and PI4K3b demonstrate the efficiency of protein knock-down by the corresponding siRNAs.

(**B**) HeLa cells were infected with RV-A16 WT (white bars) or RV-A16 2B[I92T] (black bars) were treated with DMSO, brefeldin A (BFA) or the PI4K3a inhibitor C23 (**B**), and analyzed as described in figure 1. Values represent means ± SD, n=2.

FIG. 5: Golgi disruption in RV-A16_2B[I92T] and WT infection

HeLa cells treated with DMSO or PIK93 (1 μM) were infected with RV-A16 WT or 2B[I92T] at MOI 20 for 8 h, and stained for viral protein VP1 (green) and GM130 (red). Nuclei stained with DAPI are in blue. Single z-planes from confocal imaging are shown. Scale bar is 10 μm.

FIG 6: RV-A16_2B[I92T] mutant enhances PI4P and recruits PI4P2a and PI4K3b

HeLa cells were treated with DMSO or PIK93 (1 µM), infected with RV-A16 WT or 2B[I92T] at MOI 20 for 8 h, stained for viral protein VP1 and PI4P (**A**), or PI4K3b (**C**), and nuclei were stained with DAPI. Images show single z-planes. Quantifications of perinuclear PI4P (**B**) and PI4K3b (**D**) show relative signal intensities per area from total projections with number of cells analyzed (n) and mean values and SD. Scale bar: 10 µm.

FIG. 7: RV-A16 2B[I92T] replicates at low levels of PI4K3b

(**A**) HeLa-OHIO cells were subjected to CRISPR/Cas9 knock-out with guide RNAs (gRNAs) targeting PI4K2a and PI4K3b. Knock-out was verified by Western blotting. The indicated cell lines were infected at a MOI of 20 for 8 h, and analyzed for infected cells. Values representing fraction of infected cells represent means ± SD, n=3.

(**B**) HeLa-OHIO PI3K3b KO cells were stably transfected with a doxycycline inducible PI4K3b cassette. Expression of PI4K3b was induced by different dosage of doxycycline for 24 h, and PI4K3b levels analyzed by Western blotting.

(**C**) Cells were infected with RV-A16 WT or RV-A16 2B[I92T] (MOI 20) in presence or absence of doxycycline. Progeny virus was harvested at 16 h pi, and titrated on fresh HeLa-OHIO cells.

(**D**) Cells were infected at MOI 20 in presence or absence of doxycycline and infection was assessed after 8 h and 16 h respectively. Values represent means ± SD, n=2-3.

FIG 8: PI4K 3b recruitment by the RV-A16 3A protein

HeLa cells were transfected with plasmid DNA encoding myc-tagged 2B, 2B[I92T], 3A and 3AB, stained with anti-myc antibodies (green), and with antibodies against PI4P (**A**) or PI4K3b (**B**). Nuclei were stained with DAPI. Representative single section confocal images are shown. Scale bar: 10 µm.

F1

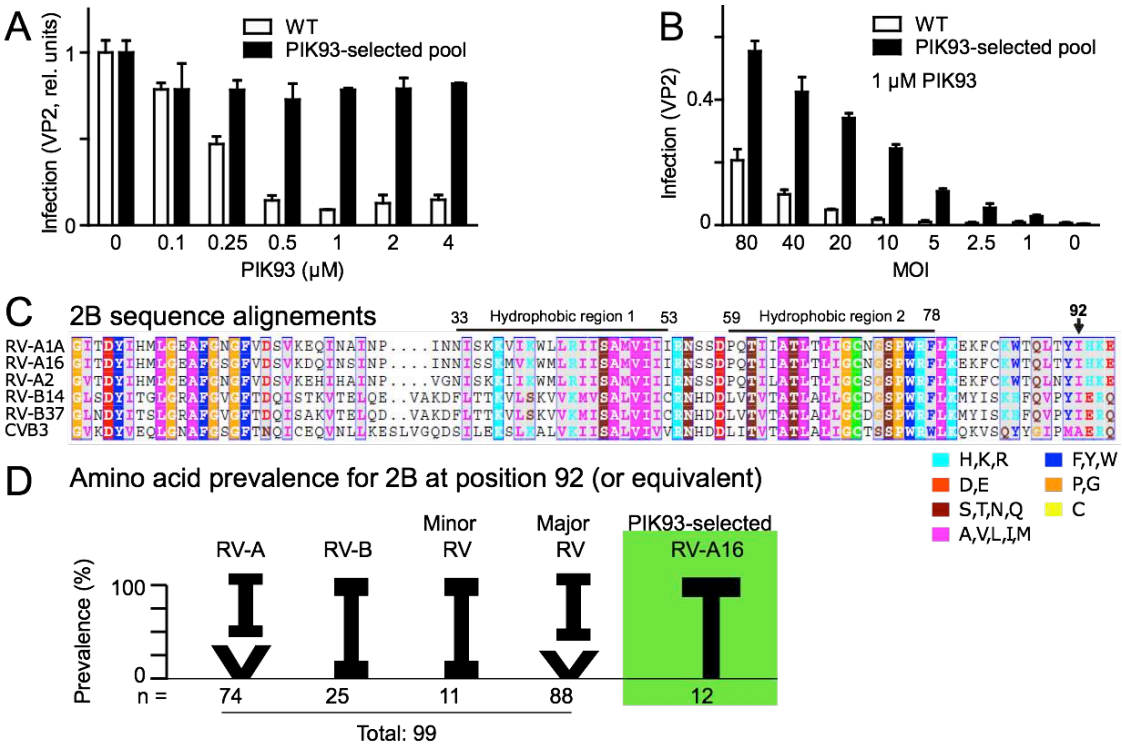
A
Infection (VP2, rel. units)
WT
PIK93-selected pool
PIK93 (μM)
B
Infection (VP2)
1 μM PIK93
MOI
C
2B sequence alignements
Hydrophobic region 1
Hydrophobic region 2
RV-A1A
RV-A16
RV-A2
RV-B14
RV-B37
CVB3
D
Amino acid prevalence for 2B at position 92 (or equivalent)
H,K,R
D,E
S,T,N,Q
A,V,L,I,M
F,Y,W
P,G
C
Prevalence (%)
RV-A
RV-B
Minor RV
Major RV
PIK93-selected RV-A16
n =
Total: 99

F2

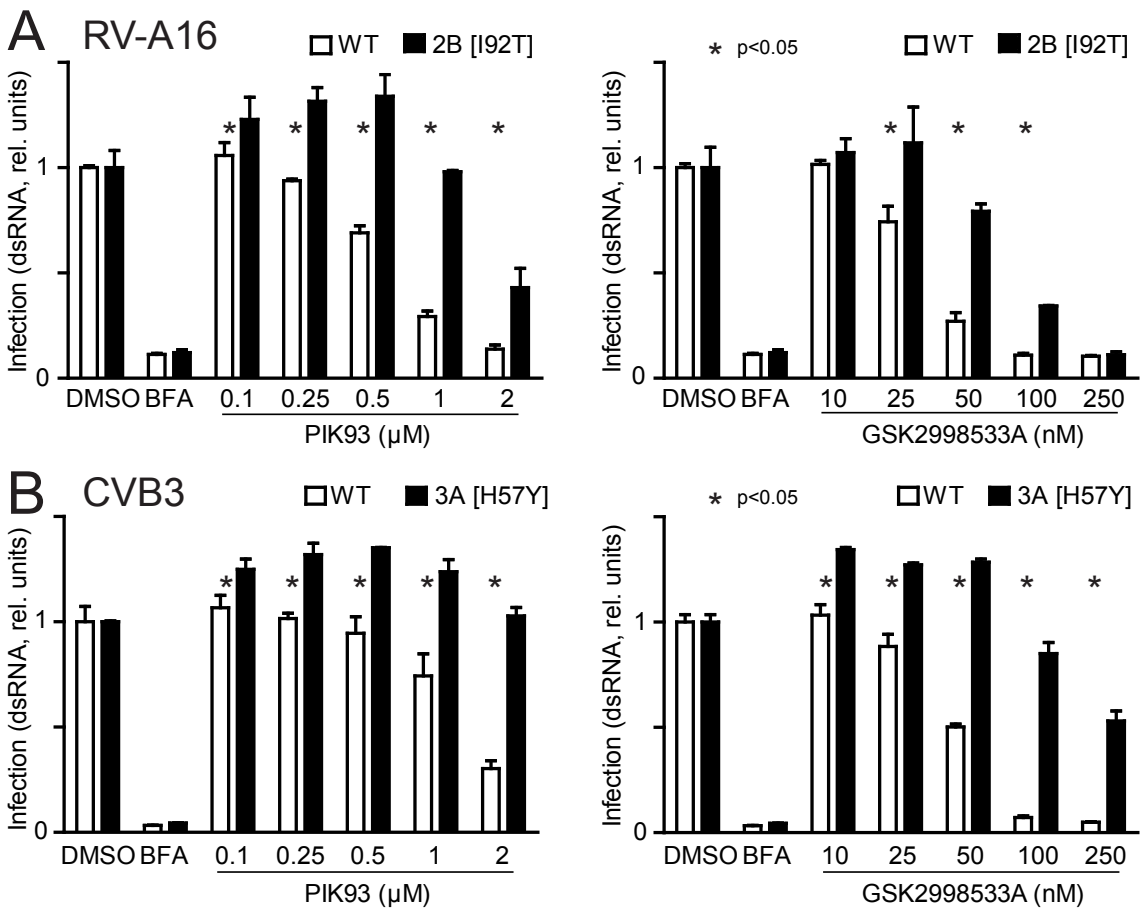
A
RV-A16
WT
2B [I92T]
Infection (dsRNA, rel. units)
DMSO BFA 0.1 0.25 0.5 1 2
PIK93 (μM)
* p<0.05
DMSO BFA 10 25 50 100 250
GSK2998533A (nM)
B
CVB3
3A [H57Y]

F3

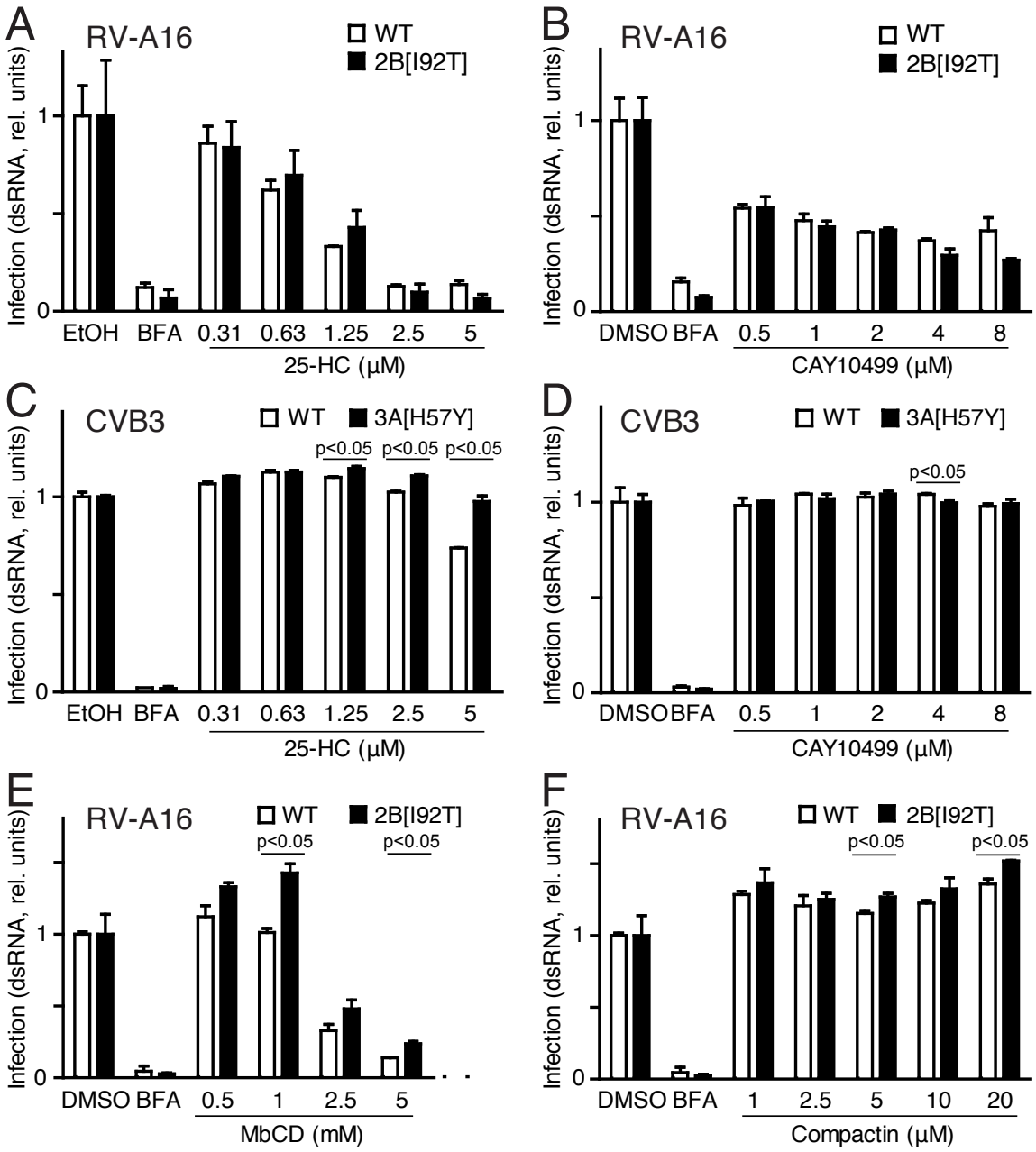
A
RV-A16
WT
2B[I92T]
Infection (dsRNA, rel. units)
1
0
EtOH
BFA
0.31
0.63
1.25
2.5
5
25-HC (μM)
B
RV-A16
WT
2B[I92T]
Infection (dsRNA, rel. units)
1
0
DMSO
BFA
0.5
1
2
4
8
CAY10499 (μM)
C
CVB3
WT
3A[H57Y]
p<0.05
p<0.05
p<0.05
Infection (dsRNA, rel. units)
1
0
EtOH
BFA
0.31
0.63
1.25
2.5
5
25-HC (μM)
D
CVB3
WT
3A[H57Y]
p<0.05
Infection (dsRNA, rel. units)
1
0
DMSO
BFA
0.5
1
2
4
8
CAY10499 (μM)
E
RV-A16
WT
2B[I92T]
p<0.05
p<0.05
Infection (dsRNA, rel. units)
1
0
DMSO
BFA
0.5
1
2.5
5
MbCD (mM)
F
RV-A16
WT
2B[I92T]
p<0.05
p<0.05
Infection (dsRNA, rel. units)
1
0
DMSO
BFA
1
2.5
5
10
20
Compactin (μM)

F4

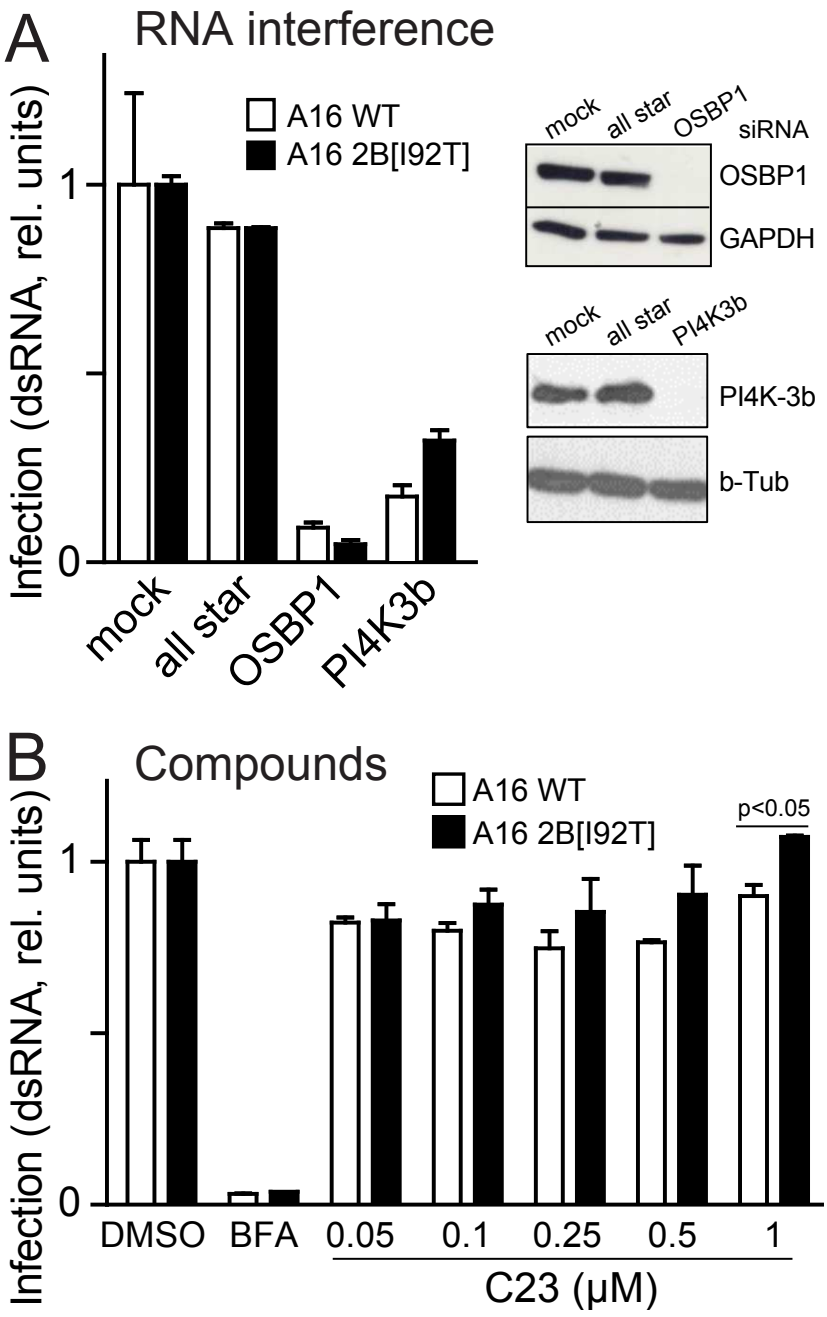
A
RNA interference
A16 WT
A16 2B[I92T]
Infection (dsRNA, rel. units)
1
0
mock
all star
OSBP1
PI4K3b
mock
all star
OSBP1
siRNA
OSBP1
GAPDH
mock
all star
PI4K3b
PI4K-3b
b-Tub
B
Compounds
A16 WT
A16 2B[I92T]
p<0.05
Infection (dsRNA, rel. units)
1
0
DMSO
BFA
0.05
0.1
0.25
0.5
1
C23 (μM)

F5

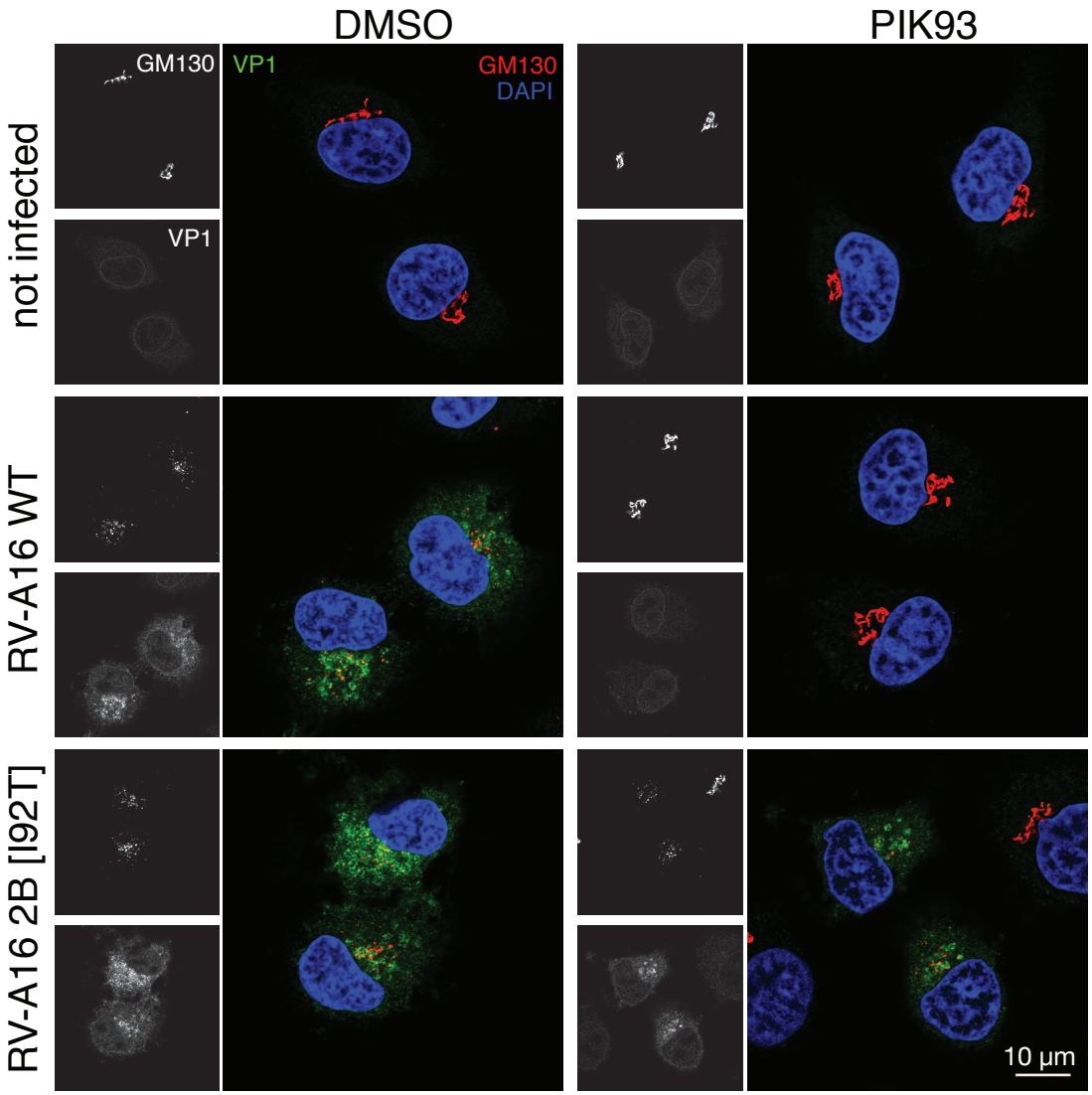
DMSO
PIK93
not infected
RV-A16 WT
RV-A16 2B [I92T]
GM130
VP1
GM130
DAPI
VP1
10 µm

F6

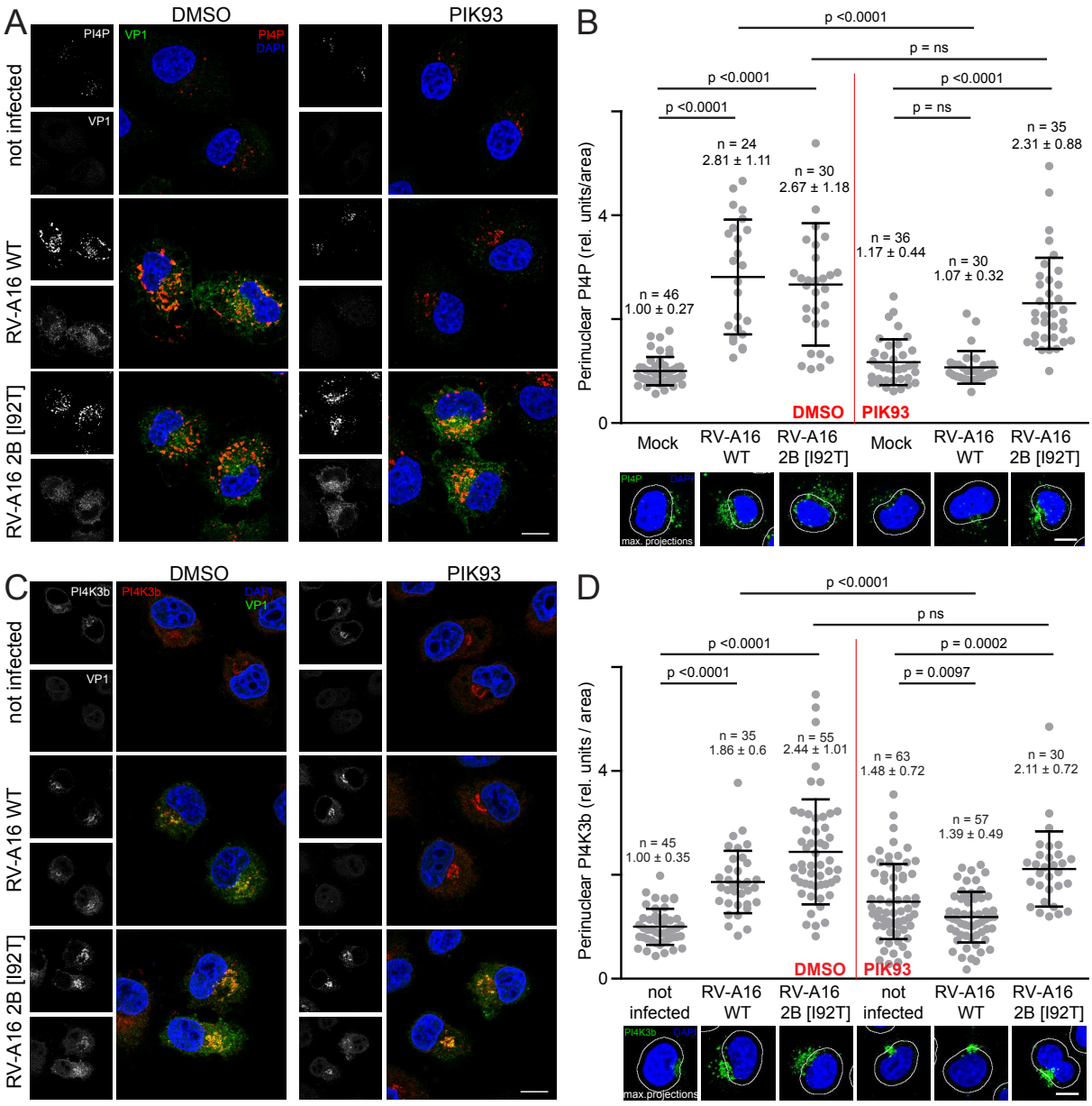
A
DMSO
PIK93
not infected
RV-A16 WT
RV-A16 2B [I92T]
PI4P
VP1
DAPI
B
p <0.0001
p = ns
p <0.0001
p <0.0001
p <0.0001
p = ns
Perinuclear PI4P (rel. units/area)
n = 46
1.00 ± 0.27
n = 24
2.81 ± 1.11
n = 30
2.67 ± 1.18
n = 36
1.17 ± 0.44
n = 30
1.07 ± 0.32
n = 35
2.31 ± 0.88
DMSO
PIK93
Mock
RV-A16 WT
RV-A16 2B [I92T]
max. projections
C
DMSO
PIK93
not infected
RV-A16 WT
RV-A16 2B [I92T]
PI4K3b
VP1
DAPI
D
p <0.0001
p ns
p <0.0001
p = 0.0002
p <0.0001
p = 0.0097
Perinuclear PI4K3b (rel. units / area)
n = 45
1.00 ± 0.35
n = 35
1.86 ± 0.6
n = 55
2.44 ± 1.01
n = 63
1.48 ± 0.72
n = 57
1.39 ± 0.49
n = 30
2.11 ± 0.72
DMSO
PIK93
not infected
RV-A16 WT
RV-A16 2B [I92T]
max. projections

F7

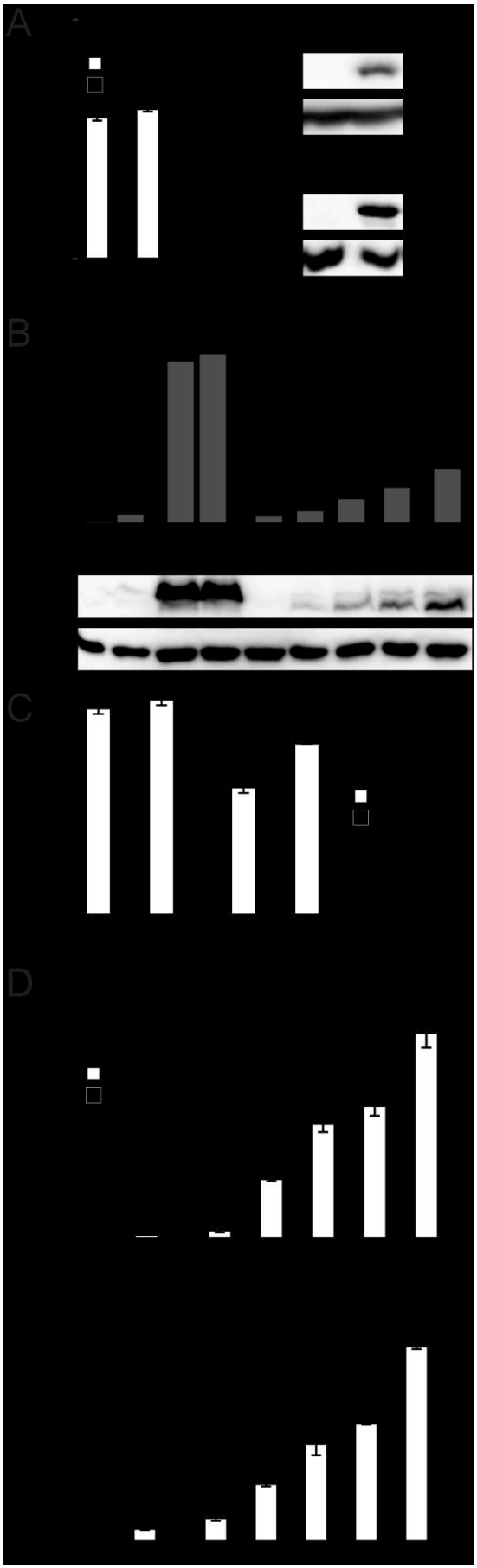

F8

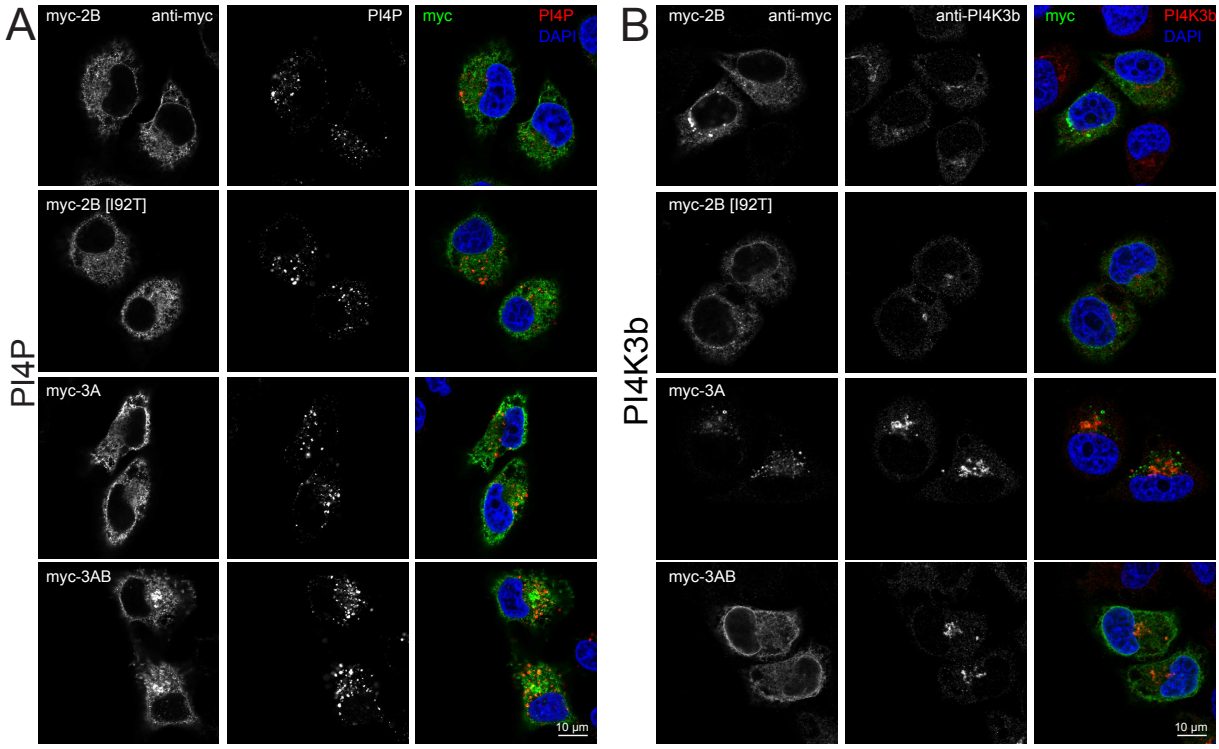
A
myc-2B
anti-myc
PI4P
myc
PI4P
DAPI
myc-2B [I92T]
myc-3A
myc-3AB
10 µm
PI4P
B
myc-2B
anti-myc
anti-PI4K3b
myc
PI4K3b
DAPI
myc-2B [I92T]
myc-3A
myc-3AB
10 µm
PI4K3b